Paper # 070MI-0368 Topic: Microcombustion and New Combustion Devices

8th U. S. National Combustion Meeting
Organized by the Western States Section of the Combustion Institute
and hosted by the University of Utah
May 19-22, 2013

The Influence of Electric Field Power Systems on Flame Behavior

Koji Yamashita[1] *Yu-Chien Chien*[2] *Sunny Karnani*[2] *Derek Dunn-Rankin*[2]

[1]*Department of Mechanical Engineering*
Aoyama Gakuin University, Tokyo, Japan
[2] *Department of Mechanical and Aerospace Engineering*
University of California, Irvine, California 92697-3975

This paper describes the effect of the electric field generated by two different high voltage power supplies on a coflowing jet flame. The paper is motivated by the increased availability of low-cost high-voltage power supplies and the question of whether their performance characteristics are suitable for flame-generated chemi-ion current measurements (nano/microamp) in sensitive environments. Economical designs, which may involve removing active current sinking components, can compromise a power supply's ability to respond on the millisecond time scales that have made the electric actuation of flames a unique approach to combustion sensing and control. The influence of several factors on the measured ion current, including rise time to a desired set point, precision and drift of the applied voltage, and voltage ripple, are important. Experiments are conducted using a small coflowing jet flame and two different power supplies; one supply is a high performance laboratory grade device and the other an inexpensive compact and lightweight unit. Methane is selected as the fuel source in order to reduce the potentially confounding influence of soot. Flame behavior is characterized optically and by the measured ion current. Optical measurements show the flame response and the response of the surrounding thermal field.

1. Introduction

Utilizing electric fields is one of the interesting methods available to change flame behavior on short timescales. Electric fields have been shown to affect soot formation and transport, flame character, stabilization and extinguishment [1-3]. Under the conditions where the flame is strongly influenced by the electric field, it is likely that the involved electrical components, such as the power supply, need to have adequate capabilities with respect to the flame response.

The flame has electrical character because of charge carriers created during chemical combustion reactions. For example, H_3O^+ is the most dominant charged specie that can survive the reaction zone when an external field is applied; it has much higher concentration than other ions such as $C_2H_3O^+$ and $C_3H_3^+$ in hydrocarbon flames [4]. Negative charge carriers in flames are mostly electrons but once leaving the flame may attach to other molecules and form negative ions. Electrons do not play a major role in the electrical actuation of flames because the high mobility limits the body force applied to the neutral gas. When placed in an electric field, charged species accelerate along a gradient towards the electrode of opposite polarity. The increased kinetic energy, which results from

electric field work over each mean free path, is transferred to neutral molecules through collisions, Charged particles therefore continuously lose and regain kinetic energy. The net direction of ion drift is from positive to negative polarity when positive ions are dominant in the flame. This ion behavior is sometimes called "Ion driven wind" [5].

The ion driven wind in small flames is on the order of meters/second and so it is confounded by natural convection under 1g conditions [6]. For this reason, micro- or zero-gravity experiments are desirable to investigate this subject. The Advanced Combustion via Microgravity Experiments (ACME) project of NASA encompasses a group of non-premixed flame experiments that require a microgravity environment. The E-FIELD experiment, within the ACME project, is focused on understanding and utilizing electrical effects of flames. In preparation for operation of E-FIELD aboard the International Space Station, this paper explores the similarities and differences between flame behavior when actuated by a typical laboratory high-voltage power supply and a lightweight compact power supply that is suitable for use in spaceflight experiments. In particular, there are some open questions regarding the relationship between temporal response of the power supply generating the potential gradient between the electrodes and that of the flame behavior. As mentioned earlier, micro- or zero-gravity experiments are needed for absolute certainty on this subject, but this paper begins to explore this relationship in the 1g laboratory environment. The paper compares the response of two power systems and the effects of that response on a small co-flow diffusion methane/air flame. The comparison includes measurements of voltage, ion current, and flame shape.

2. Methods

A co-flow burner is used for creating a small diffusion flame. It is produced with two stainless-steel double cylinders. The inner diameter is 2.13 mm and the outer diameter is 25 mm. The fuel flows through the inner tube. Air goes into the outer tube through a honeycomb mesh which is installed at the outlet in order to make the airflow more uniform. Further details on the burner can be found in [8]. A schematic of the experiment is shown in Figure 1.

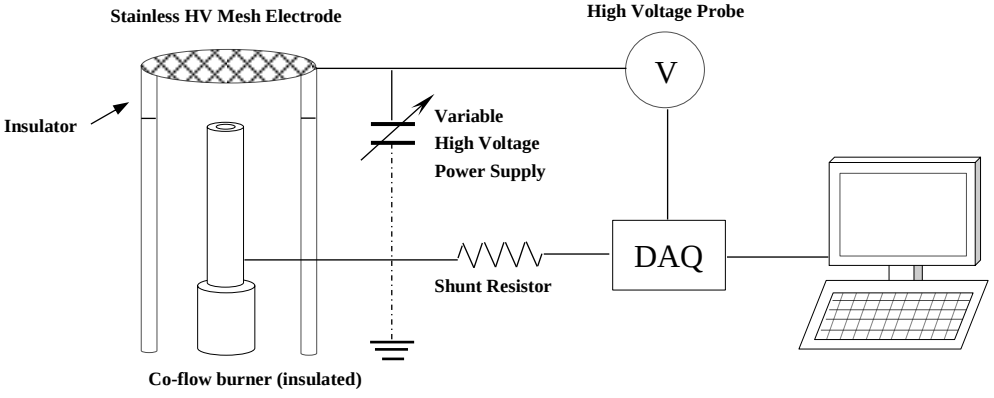

Figure. 1 Experimental schematic

Applying a large potential difference between the burner and a wire mesh 2.5 cm above the burner creates the electric field. The burner and mesh are insulated and isolated electrically. The field strength E is approximately determined as E=V/d [kV/cm] where *d* represents the distance between the mesh and the top of the burner. The potential drop across a shunt resistor, placed between the

burner and electric ground, is measured and related to ion current using Ohm's Law. Two high voltage power supplies are used in the comparison: A high performance laboratory grade device (TREK Model 609A-3) and an inexpensive compact and lightweight unit (UltraVolt HVPS Models 20A12-P4-F-M-C-AS and 20A12-N4-F-M-C-AS). Both supplies have a -10 kV to +10 kV voltage range. The UltraVolt power supplies are planned for the electric field combustion experiment in the ACME project. High-speed flame movies are taken with a Casio EX-F1 camera.

3. Results and Discussion

Power supplies capabilities

Figure 2 shows the power supply response time when large and small step inputs are requested: (a) asking for maximum output voltage from minimum output voltage (i.e. -10 kV - +10 kV), (b) asking for a 100 V step from 0 V. It should be noted that both responses have an approximately 4 ms delay between the request and reaction. This constant delay is the time that the control voltage needs to respond. In Fig. 2(a), the TREK shows that the output voltage rises almost vertically and immediately reaches the requested voltage with a small overshoot while the HVPS voltage rises slowly after the control voltage is applied. This curve asymptotically approaches the requested voltage. The HVPS requires time to respond between its own two supplies, one generating positive and the other generating negative voltage. Small fluctuations can be seen in the positive output region. In Fig. 2(b) with a small step request (100 V), the HVPS has quite a large ripple with an amplitude equivalent to the requested voltage.

The comparison of the rise time is a typical way to discuss the system response. In this paper, the rise time is defined as the time between 10% to 90% of the step height, which means -8 kV to +8 kV in those systems for the largest voltage step. The TREK response is on the order of milliseconds, while the HVPS takes approximately 100 ms.

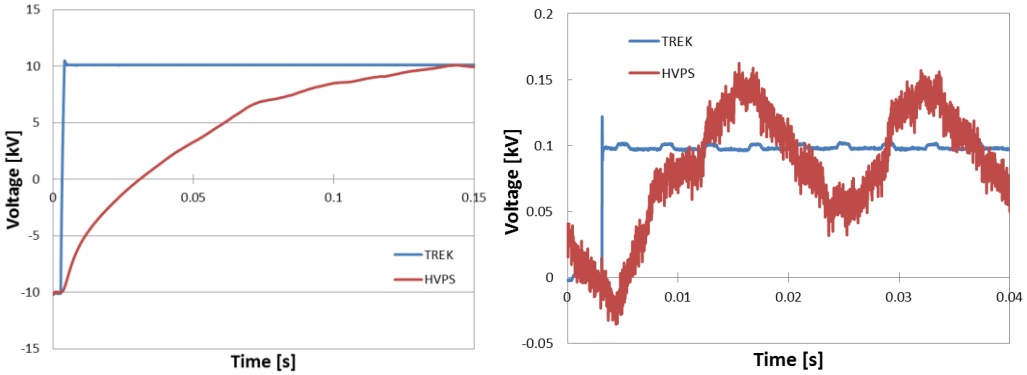

Figure. 2 Electric response to a step input for both supplies; (a) large step: -10kV to 10kV, (b) small step: 0V to 100V

Figure 3 shows the ramp response using a 1kV square wave signal with different cycle time, 200 ms, 100 ms and 50 ms respectively. The HVPS has an approximately 200 V overshoot before settling to the 1 kV request voltage. On the TREK side, the overshoot is much smaller and can be neglected (about 10 V). The HVPS maintains agreement with the requested voltage for 200 ms and 100 ms cycles, and the response starts delaying for 50 ms steps. The TREK is able to work with accurate response for nearly all conditions.

Figure 4 illustrates the voltage response when stepping up and down the request voltage in 500 V increments between 5kV and 0V (in a large triangle profile). This series mimics what will be a voltage-current characteristic curve sweep in the E-FIELD experiment. The steps are taken at higher frequency than the square wave according to the narrower stepping increment; Figure 4 (a_1), (b_1), and (c_1) show results with steps of 20 ms, 10 ms, and 7.5 ms each cycle; and (a_2), (b_2), and (c_2) show the same results but focused near the peak of the triangle profile. With the requested step getting smaller, the HVPS responds slower with higher cycle rates. The voltage overshoots and starts to fall before the value has converged to the request value; the step shape is no longer a square in (b), and (c). The TREK can reach the requested voltage, and its value converges immediately. Its voltage is a little higher than the requested voltage but the difference is not significant. The TREK can safely be used, therefore, as the ideal response case system for comparison.

As mentioned before, the HVPS shows good agreement on 100 ms timescales. However, this timescale is approximately the same as that associated with the buoyant flows, making it difficult in 1g to distinguish the effects of the power supply and that of the flame.

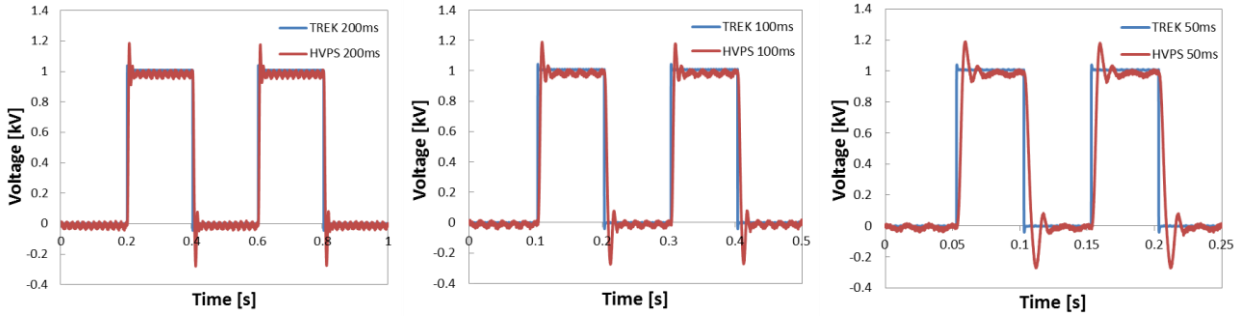

Figure. Three 1kV square wave with different cycles; (a) 200ms, (b) 100ms and (c) 50ms

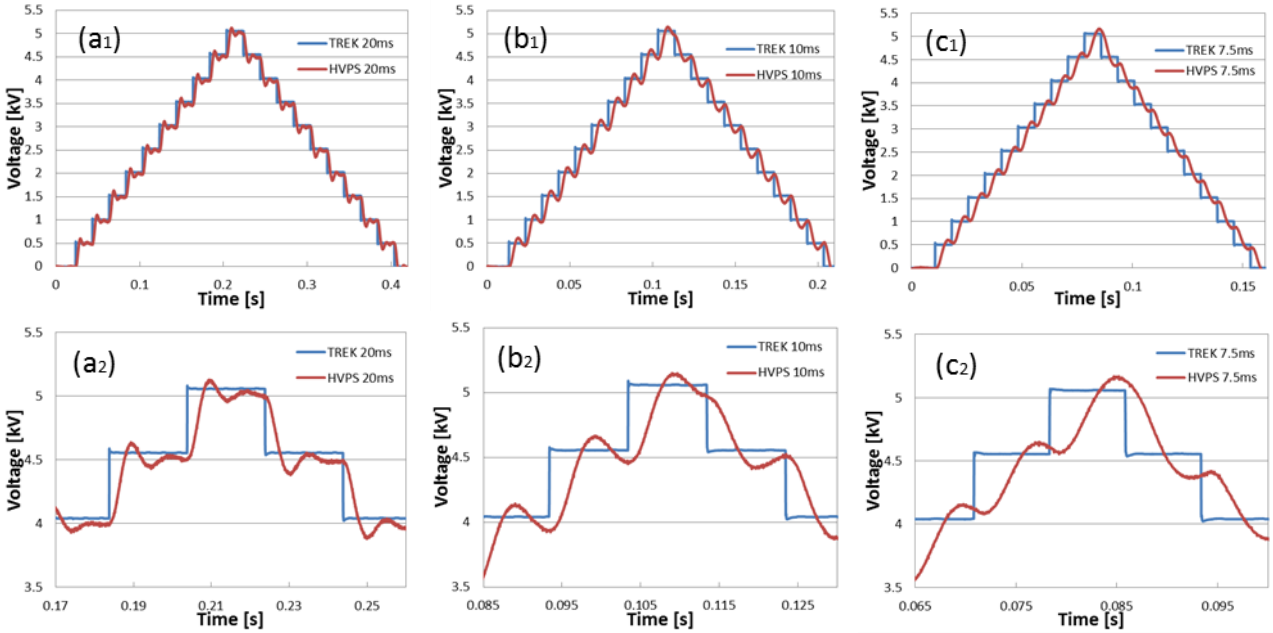

Figure. 4 500 V step response asked for 5kV and back to 0 V with different cycles; (a_1) 20 ms, (b_1) 10 ms, and (c_1) 7.5 ms and (a_2), (b_2), and (c_2) are detailed portion from above.

Ion current

Before discussing the ion current, the direction of the electric field needs to be defined. The high voltage power supply is wired to an insulated and isolated mesh above the burner. The output voltage is applied on the mesh, making the mesh the active potential surface. The burner is also isolated from the surroundings but it is kept at zero potential. For this reason, the definition of the polarity is based on the voltage applied to the upper mesh in this paper. Because of the presence of charged particles in the combustion field, a flame and its neutral gas surroundings can be regarded as a complex electrical resistor. The ion current is one of the significant characteristics describing the flame in an electric field since it reflects the resistance to current flow at a given voltage. The saturation ion current for the small diffusion flame in this set of experiments is on the order of a few microamps.

The measured steady ion current with five different flow conditions are shown as VCC (Voltage-Current Characteristic) curves in Figure 5, where (a) represents the entire data set, and (b) and (c) represent detailed positive and negative regions, respectively. The figure shows the typical distinct three regions of the ion current behavior in a flame. At first, the ion current rises (or falls) following a quadratic curve with increasing field strength. Then it reaches a plateau region and stops rising. With increasing field strength, the ion current rises again, following a parabolic curve until the flame blows off (upward directed ion driven wind – negative mesh) or is extinguished (downward directed ion driven wind – positive mesh). Those three regions are called the subsaturation region, the saturation region, and the supersaturation (or secondary ionization) region, respectively. The supersaturation region is often complicated by corona discharge effects from the burner and mesh so it often better to avoid the extreme voltages when trying to understand the electrical aspects of the flame alone.

The results in Figure 5 demonstrate that both supplies correspond to each other in the saturation region. However, there are considerable differences in the other regions. The ion current measured using the HVPS rises (or falls) with smaller field strength in the subsaturation and supersaturation regions. Therefore transition points in between the regions appear at lower field strength with the HVPS. That trend is more significant under the higher flow condition. The power supplies are in good agreement with each other under the lower flow speed condition. This is a promising finding for the zero-gravity studies planned because electrical effects and their competition with buoyancy are much more pronounced when there is lower forced convective momentum.

The flame response in terms of ion current is shown in Figure 6 following a step input from 0 V to 5 kV. The initial spike observed in the TREK case corresponds to the capacitance of the burner/mesh electrode system. The current then decays to a steady value representative of the flame/electrode gap space. This phenomenon was characterized fairly extensively in [9]. The rising ion current after the initial spike is likely due to the flame finding a new accommodation with the ion driven wind. The flame then settles to a steady condition after 30-40 ms. The HVPS results show a much less prominent spike because the slower response time does not engage the small system capacitance. It is very interesting to note, however, that the settling time of the ion current, and its ultimate value matches very well the results obtained when using the TREK. The insensitivity results because the requested voltage of this measurement is in the saturation region where the ion current does not rise with electric field strength. Therefore, the electric response is largely unaffected by the power supply response time. This a fortuitous condition that provides an important opportunity to maximize the

understanding of flame behavior even when using a slow responding power supply. That is, operating with step changes between saturated regions can create more rapid response changes in the ion current than is strictly available in the voltage.

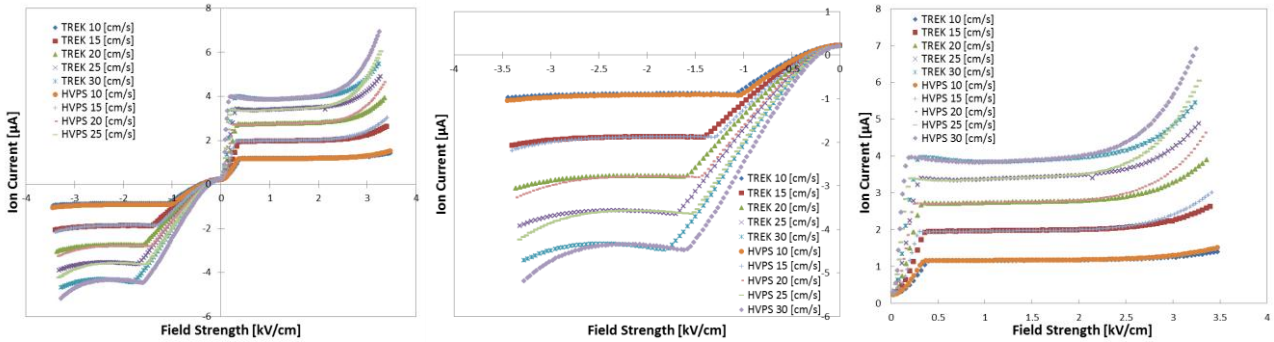

Figure. 5 VCC curve under the different flow speed conditions; (a) overall, (b) detailed negative polarity, (c) detailed positive polarity

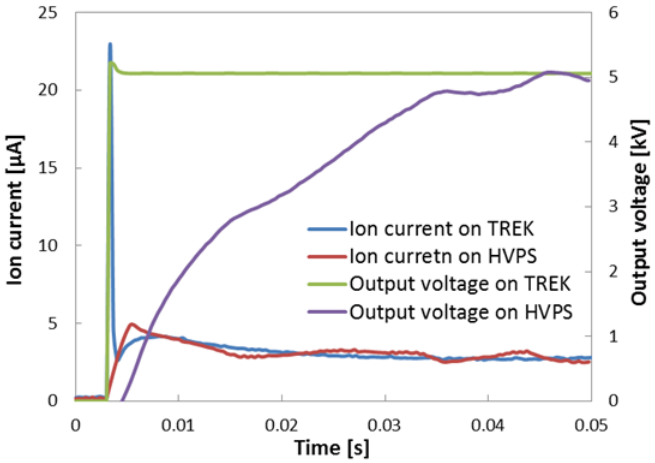

Figure. 6 Ion current response comparison asking for 5 kV step input on two supplies

Visualized flame response

While there is experimental verification that the ion current response between the two power supplies is quite similar in time, the connection between this ion current and the flame behavior is still needed. Visualized flame response following steps of voltage using the TREK and the HVPS are illustrated in Figure 7. The images are extracted from flame videos captured with a camera filming at a rate of 300 fps. Starting with an initially negative potential applied at the mesh, a positive step voltage is then applied, which produces an increasing voltage range from -9 kV to +9 kV. A LED light is placed right next to the flame to indicate when the control voltage is applied from the power supplies in order to set the zero time on the images.

The results show that the TREK takes about 20.3 ms while the HVPS takes 130 ms to reach +9 kV (Figure 7). Generally, the flame is stabilized while the high voltage is applied. When the mesh is negative, the flame is extended vertically upward, and it becomes thinner. Conversely, while the mesh is positive, a downward wind is imposed, opposing natural convection. While only qualitative, it appears from Figure 7 that with a simple time stretching the flame character matches between the two power supplies. This is slightly different from the ion current finding, which would have

indicated that the flame response time should be unaffected. The difference is that in the -9 kV to 9 kV test the step is not into a saturated ion current condition but between two conditions in the supersaturated regions. In this circumstance, there will be sensitivity in the ion current. In any case, the still images are slightly misleading, and the high speed movies show more dynamic processes. In the TREK case, for example, the video shows that the flame is stabilized just 10 ms after the polarity is reversed. The flame transitions smoothly with little fluctuation from the narrow stretched shape with the upward wind to the flattened shape with the downward wind. On the other hand, when using the HVPS, the flame takes more than 100 ms to stabilize, and it continues to exhibit oscillations. With this slower responding power supply, the flame development seems separated into two stages where the flame reacts quickly at first and then slowly widens. This behavior corresponds to the electric response of the HVPS shown in Figure 2. The high voltage ripple in the output is likely responsible for the oscillations. The ripple does not affect the steady state ion current results because they are average values. Further study is needed but the dynamic differences noted above are consistent with considering the flame an active element of the system with a response time on the order of 30 ms [10,11]. In the TREK case, the flame finds itself instantaneously facing an electric field condition that it then accommodates with a self-consistent change in shape and ion current generation. In the case of the HVPS the environment conditions (i.e., the electric field imposed) is continually changing as the flame tries to accommodate the variation. This leads naturally to a more unstable behavior, particularly when the field is coupled with the ion current response.

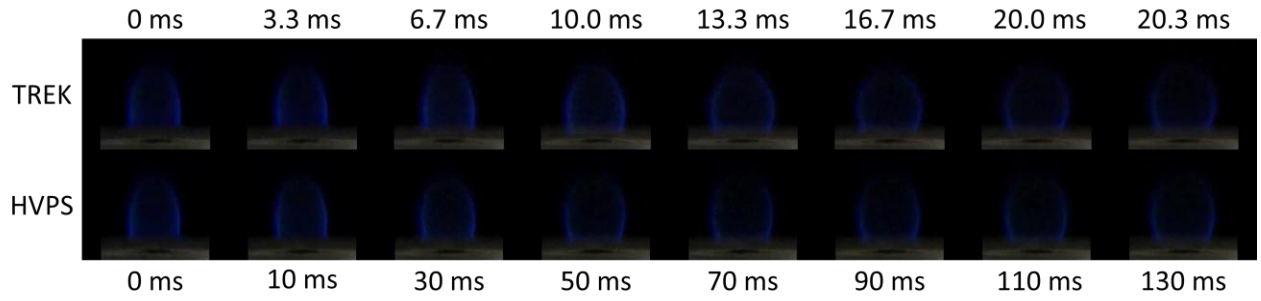

Figure.7 Flame response from -9kV to +9kV on two supplies

4. Conclusions

This work contributes to clarifying the interaction between electric forcing and flame behavior. The data helps provide information that can be used to create a transfer function between flame and electric supply system. Ultimately, the goal of this research is to describe the relationship between flames and an imposed electric field with sufficient clarity to allow active control. More immediately, the results show that there are conditions where a slower responding power supply can provide reliable performance in an electrically actuated flame system. In particular, these conditions include steady averaged VCC sweeps and step changes between saturated ion current conditions. These findings will certainly contribute to more effective use of the data to be obtained during the International Space Station ACME experiments.

Acknowledgements

This research was funded by the NASA ISS Research Project agreement NNX07AB55A with contract monitor Dennis Stocker.

Disclaimer
Product names and models are provided only for clarification and are in no way an endorsement on the part of NASA or the federal government.

References
1. J. Kuhl, G. Jovicic, L. Zigan, and A. Leipertz. Study of laminar premixed flame in transient electric fields using PLIF and PIV techniques. 16th International Symposium on Applications of Laser Techniques to Fluid Mechanics, July 09-12 2012.

2. Y. Wang, G. Nathan, Z. Alwahabi, K. King, K. Ho, and Q. Yao. Effect of a uniform electric field on soot in laminar premixed ethylene/air flames. Combustion and Flame, 157(7):1308–1315, 2010.

3. S. Won, S. Ryu, M. Kim, M. Cha, S. Chung, "Effect of electric fields on the propagation speed of tribrachial flames in coflow jets" Combustion and Flame, 152, 496-506, 2008.

4. T. Pedersen and R.C. Brown, (1993) "Simulation of electric field effects in premixed methane flames" *Combust. Flame*, 94, 433–448.

5. J. Lawton and F. J. Weinberg, (1969) "Electrical Aspects of Combustion" Clarendon Press. Oxford.

6. S. Karnani, D. Dunn-Rankin, F. Takahashi, Z.-G. Yuan, and D. Stocker. Simulating gravity in microgravity combustion using electric fields. Combustion Science and Technology Special Issue: The 23rd International Colloquium on the Dynamics of Explosions and Reactive Systems, 184(10-11), 2012.

8. S. Karnani, and D. Dunn-Rankin, "Electric field effects on a small co-flow diffusion flame" In Proceedings of the 6th U.S. National Combustion Meeting, Ann Arbor, MI, May 17-20, 2009.

9. F. Borgatelli, and D. Dunn-Rankin, (2006) "Feedback Control of Ion Current from a Small Diffusion Flame," Paper 06S-44, Western States Section/The Combustion Institute Spring Meeting, University of Idaho, Boise, March 27--28.

10. M.J. Papac, and D. Dunn-Rankin, "Modeling Electric Field Driven Convection in Small Combustion Plasmas and Surrounding Gases," Combustion Theory and Modeling, 2007.

11. F. Borgatelli, D. Dunn-Rankin, "Behavior of a small diffusion flame as an electrically active component in a high-voltage circuit" Combustion and Flame, 159, 210-220

12. Y.C. Chien, D. Dunn-Rankin, "Electric Field Effects on Carbon Monoxide Release from Impinging Flames", 8th US National Combustion Meeting, 2013